

Published in final edited form as:

*Anal Chem.* 2002 August 15; 74(16): 4054–4059.

## A Chip-Based Electrophoresis System with Electrochemical Detection and Hydrodynamic Injection

Ulli Backofen<sup>†</sup>, Frank-Michael Matysik<sup>‡</sup>, and Craig E. Lunte<sup>†</sup>

Department of Chemistry, University of Kansas, Lawrence, Kansas 66045, and Institut für Analytische Chemie, Universität Leipzig, Linnéstrasse 3, 04103 Leipzig, Germany

### Abstract

A simple capillary electrophoresis system in the planar format that uses a new, hydrodynamic injection principle is described. The system was realized with poly(dimethylsiloxane)–glass chips and microdisk electrodes for amperometric detection. Using a double-tee injector, no precise voltage control of the electrolyte reservoirs was needed, thus making the microchip CE system more user-friendly. The analytical characteristics of chip-based CE-EC were evaluated using ascorbic acid as the model analyte. The reproducibility of migration time and signal height was expressed by relative standard deviations of 1.2% and 5.1%, respectively ( $n = 5$ ). The limit of detection for ascorbic acid was  $\sim 5 \mu\text{M}$  at a signal-to-noise ratio of 3. Practical application concerning the determination of physiologically relevant compounds such as noradrenaline and L-dopa are discussed.

In recent years, there has been a significant interest in miniaturized analytical systems. The downscale in electrophoresis results in a decrease in analysis time and a potential increase in efficiency while the instrument becomes more compact due to integration of essential parts onto a single substrate.<sup>1,2</sup> Another attractive feature is the possibility of parallel analysis using multiple separation systems residing on one chip. Capillary electrophoresis (CE) in the planar format has been applied to a variety of analytes, e.g., DNA,<sup>3,4</sup> neurotransmitters,<sup>5,6</sup> explosives,<sup>7</sup> and the bioassay of clinically relevant compounds.<sup>8</sup> Fabrication of microfluidic devices in poly(dimethylsiloxane) (PDMS) by soft lithography provides a fast, inexpensive route to devices that can handle aqueous solutions.<sup>9</sup> These soft lithographic methods are based on rapid prototyping and replica molding and are easily accessible to chemists and biologists working under benchtop conditions.

Crucial in chip-based CE is the reproducible introduction of well-defined sample zones in the separation channel and the detection of narrow bands. While detection schemes, such as electrochemical detection (EC) or laser-induced fluorescence (LIF), can be adapted from conventional CE, sample introduction requires a completely new approach.

In microchip CE, injection is usually performed by electro-kinetic methods. The introduction of a well-defined sample plug is achieved through the channel network, i.e., a sample-guiding channel that intersects the separation channel. The first CE chips employed a tee-injector design.<sup>10</sup> Due to difficulties in the control of the sample plug, other injector layouts were developed. Improved control of the sample plug can be gained by using a cross<sup>11</sup> or double-tee injector,<sup>12</sup> which works well for the analysis of DNA using polymer sieving media.<sup>3,4</sup> For injection, an electric field is applied across the sample reservoir and

Correspondence to: Craig E. Lunte.

<sup>†</sup>University of Kansas.

<sup>‡</sup>Universität Leipzig.

the sample waste reservoir. The resulting analyte stream is perpendicular to the separation channel. In the separation phase, an electric field is applied across the separation channel. The sample plug, residing in the channel intersection, is transported toward the detector, which is placed downstream in the separation channel. For the separation of species with a much higher diffusion coefficient than DNA in sieving media, such as many pharmaceuticals in aqueous buffers, permanent voltage control of all reservoirs is necessary in order to counteract diffusion of analyte molecules into the separation channel during electrophoresis. An injection scheme that controls the voltage during both the injection and separation phases is known as pinched injection<sup>13–15</sup> and is nowadays frequently applied. To calculate the junction potential at the channel intersection, the resistance in all channels must be known. However, for the analysis of samples with a varying matrix, this is unfavorable because the resistance may change due to changes in the electrolyte composition. Furthermore, sample throughput is restricted by the excessive time needed to fill the sample channel, which is typically the same amount of time needed for separation.

A very fast injection scheme was developed in Ramsey's group.<sup>16</sup> Two separate streams of liquid, which make a 90° turn at the injector cross, are established on the chip at the same time. The mixing of both streams at their interface is prevented by continuous electroosmotic pumping of analyte from the sample reservoir to the sample waste reservoir and of background electrolyte from the run buffer reservoir to the point of detection. Injection of a small aliquot of analyte is accomplished by floating the potential at the sample reservoir and sample waste reservoirs for a short period of time, typically 0.1–0.5 s. Unlike in pinched injection, virtually no time is needed for the analyte to migrate from the sample reservoir to the injector. However, gated injection depends on fluidic behavior that cannot always be precisely controlled when complex samples of unknown origin are injected, and it is biased by the migration rate of the analyte molecules.

Manz's group found that leakage in microchip CE is substantially reduced when the layout of the chip consists of narrow sample channels. Resolution, column efficiency, and sensitivity were significantly improved without voltage control. Even the use of tee injectors was possible, thereby reducing the number of liquid reservoirs.<sup>17</sup>

Detection in CE requires fast and sensitive detectors with minimal dead volume. UV detection, which is standard in commercial CE apparatus, cannot be applied to chip CE because of its lack of sensitivity. Among the detection schemes that have been successfully combined with conventional CE, EC appears to be particularly suitable for CE in the planar format for five reasons: (i) Amperometric electrodes can be easily miniaturized without compromising detection limits, (ii) the small dimensions of microelectrodes allow for the construction of detectors with minimal dead volume, (iii) amperometric electrodes have a very short response time, (iv) preparation methods of the working electrode are compatible with planar technology, and, last, (v) the signal from an electrode does not need to be converted into another physical parameter for electronic registration. To fully exploit the potential of EC, effects of the high-voltage field on the detection circuit must be effectively minimized. This can be done by a decoupler that connects the separation voltage to ground before the channel outlet. In this approach, the working electrode (in conventional CE typically a carbon fiber) is usually inserted into the separation capillary, forming a detector cell with good collection efficiency.<sup>18,19</sup> In end-column detection, the working electrode, e.g., a microdisk electrode, is placed just outside the channel outlet.<sup>20</sup> Therefore, only a minor effect of the separation voltage on the detection system is encountered. A good signal-to-noise ratio is obtained by the unique characteristics of hydrodynamic microelectrodes employed in wall-jet detector configuration.<sup>21</sup> Since this approach circumvents the need for a special decoupler device, therefore making the chip easier to manufacture, it has been

avored by many groups for CE-EC in the chip format and applied to a variety of analytes. 5,6,8,22–25

In this paper, we present a simple chip CE system that employs a novel injection protocol and an electrochemical detector. The injection procedure is fast and reproducible and does not require precise voltage control of electrolyte reservoirs. Metal and carbon microdisk electrodes were used for amperometric detection, realizing absolute detection limits in the (sub)femtomole range.

## EXPERIMENTAL SECTION

### Chip Design and Fabrication

The layout of the CE chip with a forklike arrangement of the channels is schematically shown in Figure 1. The equally long side channels connect the run buffer reservoir (RB) and the sample waste reservoir (SW) with the injector intersection. The shorter channel, which has a much lower flow resistance because of its length, serves as connection to the sample reservoir. The channel depth of 10  $\mu\text{m}$  was uniform for the whole chip. This low channel depth and the long side channels were selected in order to minimize hydrodynamic flow induced by differences in the levels of the electrolyte in the reservoirs.<sup>13,17</sup>

The method used to create channels in PDMS is based on procedures published in the literature.<sup>25–27</sup> It involves three steps: first, the chip layout was created with a computer design program (Freehand, PC version 8.0, Macromedia, Inc., San Francisco, CA). Photomasks were exposed and developed at Lasergraphics Inc. (Lawrence, KS) at a resolution of 2400 dpi. In the second step, a master for PDMS molding was prepared. A 4-in. silicon wafer was first thoroughly cleaned and then coated with SU-8 50 negative photoresist using a spin coater (Brewer Science, Rolla, MO). After a preexposure bake, the wafer was exposed to light through the photomask using a near-UV flood source (Autoflood 1000, Optical Associates, Milpitas, CA). Following a postexposure bake, the wafer was developed in propylene glycol methyl ether acetate. The thickness of the resulting raised structures was measured with a profilometer (Alpha Step-100, Tencor Instruments, Mountain View, CA), and a uniform height of 12  $\mu\text{m}$  of the microstructure was determined throughout the chip. In the third step, a 10:1 mixture of PDMS oligomer and cross-linking agent (Sylgard 184), which had been degassed under vacuum, was poured onto the master. After curing at 70 °C for 1 h, the PDMS was removed from the mold. Holes with a diameter of 3.5 mm for the detector reservoir and with a diameter of 4.7 mm for the other three reservoirs were created with a hole punch. Finally the chip was sealed with a microscope slide and trimmed to size with a scalpel.

### Chip Operation

**Injection and Separation**—All solutions introduced into the reservoirs were filtered through a 0.45- $\mu\text{m}$  membrane filter. The channel network of the microchip was filled by alternately applying vacuum and pressure. First, the wells of the microchip were filled with electrolyte (20  $\mu\text{L}$  of run buffer in the run buffer reservoir and the sample waste reservoir, 25  $\mu\text{L}$  of sample in the sample reservoir, and 35  $\mu\text{L}$  of run buffer in the detector reservoir). Then a 2.5-mL disposable syringe was pressed against the PDMS chip, thereby forming an airtight seal. By gently moving the plunger of the syringe up and down, the channels were flushed with run buffer for ~1 min and afterward equilibrated for 10 min under electrophoretic conditions.

Capillary zone electrophoresis was carried out in uncoated channels. Three different types of high-voltage power supplies were used (Spellman CZE 1000R, Spellman High Voltage Electronics, Hauppauge, NY; F.u.G. model HCN 7E-35000, F.u.G. Elektronik, Rosenheim-

Langenpfunzen, Germany, and two in-house-constructed power supplies (one unipolar, one bipolar, maximum voltage, 2000 V) with a circuitry based on a miniaturized high-voltage converter purchased from EMCO (EMCO, Sutter Creek, CA). Platinum wires with a length of 6 mm placed in each buffer reservoir served as electrodes for electrophoresis. Virtually no bubble formation was observed at the electrodes due to the low conductivity of the borate buffer used (10 mM; pH, 9.05). In the separation phase, one power supply was connected to the run buffer well and to the detector well with the detector always at ground potential while the second power supply was connected to the sample well and sample waste well. Electrophoretic currents were continuously monitored by measuring the voltage drop across a 10-k $\Omega$  resistor directly attached to the high-voltage source. Simple digital meters were sufficient for registering readings in the millivolt range. Injection was carried out by switching off both high-voltage power supplies for a short period of time (2–10 s). Immediately after turning off the high voltage, the injector region, including a fraction of the side channel to the run buffer reservoir and a fraction of the separation channel, was filled with sample solution due to the hydrodynamic flow created by the higher electrolyte level in the sample reservoir and the short length of the channel connecting the sample reservoir to the injector. The injection process was completed, and the separation was started by synchronously turning on both high-voltage sources.

A video sequence of the injection process was recorded using a microscope (Axiolab A, Carl Zeiss, Thorngood, NY) equipped with a 50-W HBO Hg arc lamp assembly with fluorescein line filters for fluorescence measurements and a Microimage video system (Microimage video system A209 color video camera with CCU 209 camera control unit, Microimage Video Systems, Boyertown, PA). The hardware and software for capturing the video signal was purchased from Scion Corp. (Frederick, MD).

**Electrochemical Detection**—The arrangement of the working electrode used in this study is schematically shown in Figure 2. The voltammetric cell comprises a total of three electrodes for the detection and grounding of the separation circuit.

Amperometric detection was performed in the three-electrode format using either a LC-4CE potentiostat (Bioanalytical Systems, West Lafayette, IN) or a voltammetric analyzer model Autolab (Eco Chemie, Utrecht, The Netherlands) equipped with a low-current amplifier module (ECD). The working electrodes used in this study were microdisk electrodes prepared from fine metal wires (25  $\mu\text{m}$ ) and carbon fiber (30  $\mu\text{m}$ ). The electrode material was sealed into a glass tube with a prepulled conical tip (tip diameter, 0.5 mm). The working electrode was positioned at the orifice of the separation channel by means of a micropositioner (Newport). The electrochemical cell was completed by a quasi reference electrode (a coil with a diameter of 3 mm made from silver wire) and a piece of platinum wire (0.5 mm; 6 mm long) serving as the auxiliary electrode as well as the ground electrode for the separation voltage.

## Reagents and Materials

The following chemicals and materials were used as received: SU-8 50 photoresist (MicroChem Corp., Newton, MA), propylene glycol methyl ether acetate (Aldrich), 4-in. silicon wafers (test grade, Silicon Inc., Boise, ID), Sylgard 184 (Fisher Scientific), float glass (Kennedy Glass, Lawrence, KS), wire for the construction of electrodes (Good-fellow, Cambridge, U.K.), carbon fiber (Avco Specialty Materials, Lowell, MA), and microscope slides (Fisher Scientific). Boric acid, fluorescein, potassium dichromate, and sodium chloride were obtained from Fisher Scientific. The organic model analytes noradrenaline, L-dopa, and ascorbic acid were purchased from Sigma.

## RESULTS AND DISCUSSION

### Hydrodynamic Injection in CE in the Chip Format

Figure 3 shows a sequence of three photographs of the double-tee injector taken during the injection procedure. In Figure 3a, an injection potential of 1 kV is applied across the sample and the sample waste well and a second power supply is used to apply a separation potential across the run buffer well and the detector well. The two resulting streams of electrolyte are spatially well-confined by a sharp boundary at the 90° turn from the sample channel into the sample waste channel, while the double-tee region is filled with run buffer. As soon as the two separate high-voltage sources are turned off, the injector is loaded with sample (Figure 3b). A slightly higher level in the sample well in combination with a shorter length of the sample channel to the double tee creates a hydrodynamic pressure big enough to propel sample solution in the sidearm toward the run buffer well as well as into the separation channel. The sidearm is filled with slightly more sample than the separation channel due to a higher back pressure from the detector reservoir. When the two high-voltage power supplies are turned on again, a defined sample plug is introduced into the separation channel and the sample solution is pulled out of the short double-tee segment into the sample waste well (Figure 3c). The applied voltages during each step are listed in Table 1.

The injection/separation protocol described above works for the analysis of cations and slowly migrating anions. However, for small and highly charged anions, the separation voltage has to be reversed. Additionally, for electrochemical detection, it must be taken into account that the electrode in the detector cell must constantly be maintained at ground potential. To minimize the number of high-voltage power supplies used, a negative source was connected to the separation channel with the anode at ground potential and a positive source was connected to the injection channel with the cathode inserted into the sample well. Using this injection methodology, chloride and dichromate could be reproducibly injected and baseline-resolved peaks ( $t_{\text{mig}} \text{Cl}^-$ , 51 s;  $t_{\text{mig}} \text{Cr}_2\text{O}_7^{2-}$ , 62 s) amperometrically detected by means of a Ag-microdisk electrode set at 0.05 V versus Ag-quasi reference electrode.

The ratio of the voltage across the separation channel to that across the injection channel and the injection time were studied in detail using the previously described injection protocol.

#### **Ratio of the Voltage across the Separation Channel to the Injection Channel—**

To prevent leakage of sample into the separation channel, the ratio of the voltages across the separation channel and injection channel was varied. As can be seen from Figure 4, an increased background current was registered for voltages higher than 700 V applied to the injection channel (1 kV was applied across the separation channel). Obviously, at this voltage, sample solution begins to leak into the separation channel. Further increase of the injection voltage leads to more severe leakage, and sample solution almost completely broke through at a voltage above 800 V. The injection voltage also affects the peak height. To perform chip analysis at optimal sensitivity and to prevent leakage, injections were performed at 500 V.

**Injection Time—**In hydrodynamic injection, the amount of sample introduced into the separation channel depends linearly on the injection time. Figure 5 illustrates that the height of amperometrically recorded peaks correlates linearly with the injection volume. Interestingly, a 5-fold increase of the injected volume resulted in an increase in peak width of less than 20%.

**Dispersion—**Dispersion in the separation channel is often caused by phenomena such as different conductivity of the sample plug and the background electrolyte, interaction of the analyte molecules with the material of the separation channel, pressure effects,<sup>28</sup> and



excessive Joule heat. An Ohm's plot recorded for voltages ranging from 700 ( $i_{HV}$ , 1.8  $\mu A$ ) to 2000 V ( $i_{HV}$ , 4.8  $\mu A$ ) using a 10 mM borate buffer (pH 9.05) was strictly linear ( $r = 0.9992$ ,  $n = 12$ ). Therefore, dispersion caused by thermal effects can be discounted. A simple way to examine dispersion is to inject a fluorescent dye and to monitor the transport using a microscope. A solution of fluorescein ( $\sim 20 \mu M$ ) in 10 mM borate buffer (pH 9.05) injected for 7 s resulted in a sample plug of 360- $\mu m$  length. When the high-voltage power supplies were switched on, the sample plug was transported toward the detector and immediately appreciable dispersion set in. After 0.23 s, the length of the sample zone was 532  $\mu m$ , and after 0.87 s, it was 630  $\mu m$ . The rate of dispersion decreased with time. However, after 14.5 s, the sample plug was already 2.9 times longer than immediately after injection. Interactions between the chip material and the fluorescein might be a possible explanation for dispersion.<sup>13</sup> Effects caused by the high voltage applied across the injection channel are less likely as the electropherograms in Figure 4 indicate. Pressure-driven effects may also play a significant role. It was observed that slight differences in the levels in the buffer and sample wells can cause a significant flow which appears to be a particular problem in chip CE.<sup>27</sup> However, the CE chip performed reproducibly (see analytical characterization) over a period of more than 20 min, although some water evaporated from the wells, changing the liquid level.

### Electrochemical Detection in CE in the Chip Format

**Detector Arrangement**—The arrangement of the working electrode at the orifice of the separation channel is shown in Figure 2. This configuration was chosen because it allows for the placement of the electrode close to the channel outlet, thereby minimizing the dead volume of the detector, and at the same time, such placement allows easy monitoring of the position of the microdisk electrode by means of a microscope. Furthermore, in this way, the well at the channel outlet can be used as a detector cell, thereby circumventing the need for the construction of sophisticatedly sealed reservoirs.

**Effect of the Separation Voltage**—When amperometric detection principles are applied to capillary electrophoresis, special attention has to be paid to proper decoupling of the detection circuit from the separation field. To keep the CE setup simple and to avoid potential sources of band broadening, an end-column detection strategy was preferred over the use of a decoupler.

The shift of the potential applied to the working electrode (25- $\mu m$  Pt microdisk electrode) in the presence of the separation field was determined by cyclic voltammetry. A shift of 120 mV was measured when the separation voltage was set at 1 kV. Consequently, this voltage was added to the potential, which was adjusted at the potentiostat.

**Noise**—Low detection limits require a low noise level, which is related to the strategy used to separate the separation voltage from the detector. A microdisk electrode made from carbon fiber was used for the determination of the noise level because this electrode material is commonly employed for the detection of organic compounds in aqueous electrolytes in the oxidative mode. The peak-to-peak noise was typically below 1 pA when the separation voltage was set at 1 kV. A slightly higher noise level on the order of 1 pA was registered when a miniaturized high-voltage converter with a ripple of 0.25% generated the separation field. These results compare well with data obtained in conventional CE-EC.<sup>21</sup>

**Characterization of the Analytical Performance**—Ascorbic acid was used as the model compound for the characterization of the analytical performance of the chip CE-EC system. An injection of ascorbic acid with a concentration close to the detection limit is shown in Figure 6. The positive "spike" with a width of 5 s at the beginning of the

electropherogram is due to the injection process. During this period of time, the working electrode experienced a potential 120 mV higher than the potential adjusted at the potentiostat because the high voltage was turned off. However, the baseline returned to its original current immediately after the separation voltage was turned on again. The calculated limit of detection is  $\sim 5 \mu\text{M}$  at a signal-to-noise ratio of 3. The absolute detection limit is estimated to be less than 375 fg. This is more than 1 order of magnitude higher when compared to conventional CE-EC.<sup>29</sup> The calculated number of theoretical plates was 1300. Note that the sample was dissolved in 3.3 mM borate buffer, whereas the concentration of the background borate buffer was 10 mM. The reproducibility of the migration time was 1.2%, and the reproducibility of the peak height was 5.1% when five consecutive injections of 2 mM ascorbic acid dissolved in 10 mM borate buffer were performed. The small variations in peak height also reflect the good stability of the detection electrode. To maintain a reproducible performance, the sample and buffer solutions in the reservoirs had to be renewed after a period of operation of  $\sim 15$  min.

**Fast Separation of Physiological Compounds**—The separation of three biologically important compounds is shown in Figure 7. In the separation buffer used, noradrenaline is cationic, L-dopa is neutral, and ascorbic acid is anionic. All three are well resolved. From the short analysis time of 4 min (separation time of only 200 s), arise two advantages: first, noradrenaline, which is sensitive to oxidation by dissolved oxygen, does not significantly decompose during the course of analysis, and second, the time resolution of quasi-continuously monitored biological processes can be improved. Furthermore, the three consecutively recorded electropherograms displayed in Figure 7 illustrate that deactivation of the electrode and baseline drift are not issues due to the short electrophoretic run time.

## CONCLUDING REMARKS

Injection and detection in chip-based CE have been addressed in this work. Hydrodynamic injection has been introduced to an electrophoresis system in the chip format. It is applicable to cations, neutral compounds, and anions. In comparison to already established injection protocols, hydrodynamic injection is attractive because it circumvents the need for precise voltage control and is fast, instrumentally easy to implement, and not biased by the migrational behavior of the analyte molecule. A further advantage of hydrodynamic injection for detection schemes such as electrochemical detection is that the detector can always be maintained at ground potential.

Electrochemical detection with microelectrodes has been demonstrated to be easily adaptable to chip-based CE. Low absolute detection limits in the femtogram range were realized, and a good stability of the sensing electrode was observed.

## Acknowledgments

The authors acknowledge financial assistance from the National Institutes of Health (GM-49900). The authors also thank Scott Martin for much appreciated comments on the fabrication of microchips.

## References

1. Manz, A.; Harrison, DJ.; Verpoorte, E.; Widmer, HM. *Advances in Chromatography*. Brown, PR.; Crushka, E., editors. Vol. 33. Marcel Dekker; New York: 1993. p. 1
2. Kutter JP. *Trends Anal Chem.* 2000; 19:352–363.
3. Khandurina J, McKnight TE, Jacobson SC, Waters LC, Foote RS, Ramsey JM. *Anal Chem.* 2000; 72:2995–3000. [PubMed: 10905340]
4. Khandurina J, Guttman A. *J Chromatogr, A.* 2002; 943:159–183. [PubMed: 11833638]

5. Gawron AJ, Martin RS, Lunte SM. *Electrophoresis*. 2001; 22:242–248. [PubMed: 11288891]
6. Schwarz MA, Galliker B, Fluri K, Kappes T, Hauser PC. *Analyst*. 2001; 126(2):147–151. [PubMed: 11235094]
7. Wallenborg SR, Bailey CG. *Anal Chem*. 2000; 72:1872–1878. [PubMed: 10784156]
8. Wang J, Chatrathi MP, Tian B, Polsky R. *Anal Chem*. 2000; 72:2514–2518. [PubMed: 10857628]
9. McDonald JC, Duffy DC, Anderson JR, Chiu DT, Wu H, Schueller OJA, Whitesides GM. *Electrophoresis*. 2000; 21:27–40. [PubMed: 10634468]
10. Manz A, Harrison DJ, Verpoorte EMJ, Fettinger JC, Paulus A, Lüdi H, Widmer HM. *J Chromatogr*. 1992; 593:253–258.
11. Harrison DJ, Fluri K, Seiler K, Fan Z, Effenhauser CS, Manz A. *Science*. 1993; 261:895–897. [PubMed: 17783736]
12. Effenhauser CS, Manz A, Widmer HM. *Anal Chem*. 1993; 65:2637–2642.
13. Ocvirk G, Munroe M, Tang T, Oleschuk R, Westra K, Harrison DJ. *Electrophoresis*. 2000; 21:107–115. [PubMed: 10634476]
14. Alarie JP, Jacobson SC, Culbertson CT, Ramsey JM. *Electrophoresis*. 2000; 21:100–106. [PubMed: 10634475]
15. Heeren, vF; Verpoorte, E.; Manz, A.; Thormann, W. *J Microcolumn Sep*. 1996; 8:373–381.
16. Jacobson SC, Koutny LB, Hergenröder R, Moore AW Jr, Ramsey JM. *Anal Chem*. 1994; 66:3472–3476.
17. Zhang CX, Manz A. *Anal Chem*. 2000; 73:2656–2662. [PubMed: 11403313]
18. Park S, Lunte CE. *Anal Chem*. 1995; 67:4366–4370. [PubMed: 8651479]
19. Rossier JS, Ferrigno R, Girault HH. *J Electroanal Chem*. 2000; 492:15–22.
20. Matysik FM. *Electroanalysis*. 2000; 12:1349–1355.
21. Backofen U, Matysik FM, Lunte CE. *J Chromatogr, A*. 2002; 942:259–269. [PubMed: 11822390]
22. Slater JM, Watt EJ. *Analyst*. 1994; 119:2303–2307.
23. Woolley AT, Lao K, Glazer AN, Mathies RA. *Anal Chem*. 1998; 70:684–688. [PubMed: 9491753]
24. Wang J, Tian B, Shalin E. *Anal Chem*. 1999; 71:3901–3904. [PubMed: 21662891]
25. Martin RS, Gawron AJ, Lunte SM. *Anal Chem*. 2000; 72:3196–3202. [PubMed: 10939387]
26. Duffy DC, McDonald JC, Schueller OJA, Whitesides GM. *Anal Chem*. 1998; 70:4974–4984. [PubMed: 21644679]
27. Duffy DC, Gillis HL, Lin J, Sheppard NF, Kellogg GJ. *Anal Chem*. 1999; 71:4669–4678.
28. Crabtree HJ, Cheong ECS, Tilroe DA, Backhouse CJ. *Anal Chem*. 2001; 73:4079–4086. [PubMed: 11569795]
29. Olsson J, Nordström O, Nordström AC, Karlberg B. *J Chromatogr, A*. 1998; 826:227–233.



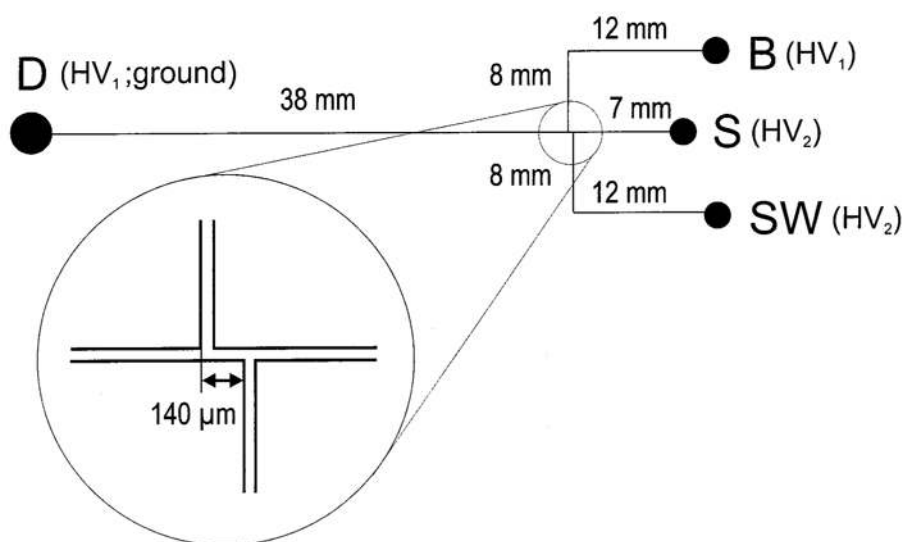


**Figure 1.** Schematic layout of the CE microchip. All channels have a uniform depth and width throughout the chip of 12 and 30 μm, respectively: D, detector; B, run buffer reservoir; S, sample reservoir; SW, sample waste reservoir; HV<sub>1</sub> and HV<sub>2</sub>, high-voltage sources.

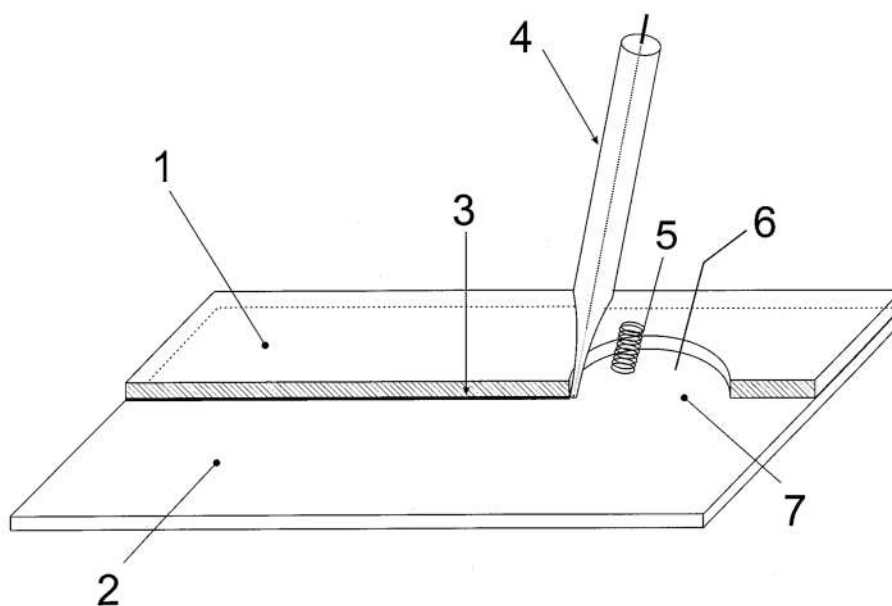


**Figure 2.** Schematic representation of the electrophoresis chip with the working electrode: (1) PDMS layer; (2) glass substrate (microscope slide); (3) separation channel ( $12\ \mu\text{m}$  deep,  $30\ \mu\text{m}$  wide); (4) working electrode ( $25\text{-}\mu\text{m}$  Pt microdisk electrode, tilted by  $15^\circ$ ) with a tip diameter of  $\sim 400\ \mu\text{m}$ . The Pt disk is placed  $200\ \mu\text{m}$  away from the orifice of the separation channel. The quasi-reference electrode (5) and the counter electrode (6) are located in the circular detector reservoir (7).

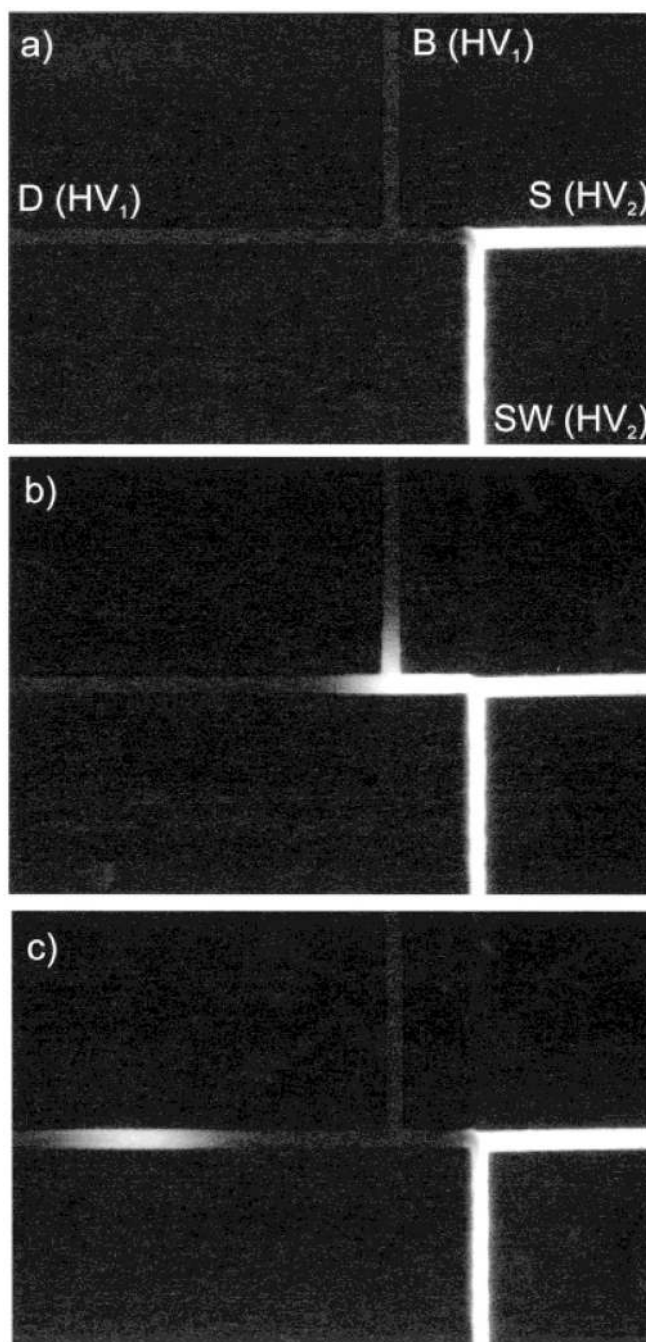


**Figure 3.** Fluorescence micrographs of the injection process. (a) The high-voltage sources  $HV_1$  and  $HV_2$  are switched on. Analyte is transported from the sample reservoir (S) to the sample waste reservoir (SW) and run buffer from the reservoir (B) to the detector (D). (b) For injection, both high-voltage power supplies are switched off for  $\sim 3$  s. (c) The sample plug is introduced into the separation channel by synchronically switching on the high-voltage sources and at the same time the two separate streams of electrolyte are reestablished.

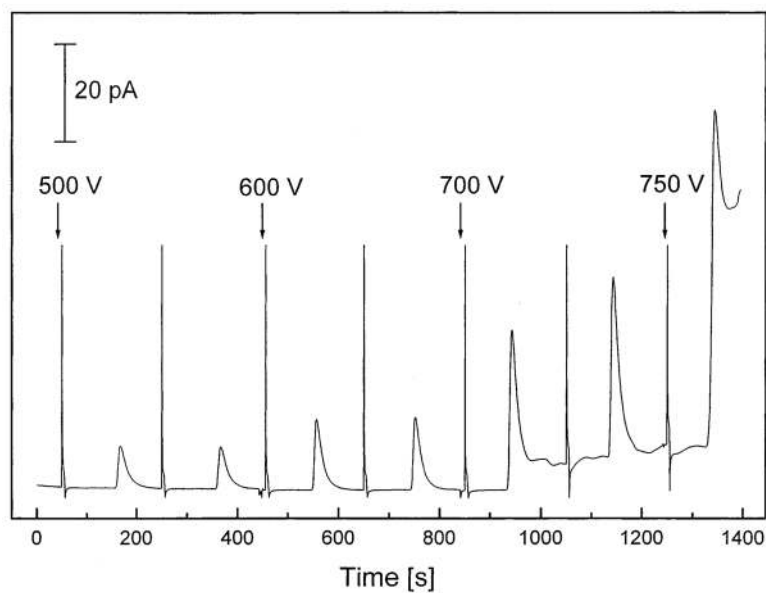


**Figure 4.** Effect of the voltage in the sample channel. The arrows indicate when a new voltage  $HV_2$  was adjusted. The spikes are due to the injection process. Experimental conditions: analyte, 1 mM ascorbic acid; background electrolyte, 10 mM boric acid;  $HV_1$  set at 1 kV; detection, carbon microdisk electrode set at 750 mV vs Ag-quasi reference electrode; injection time, 10 s.

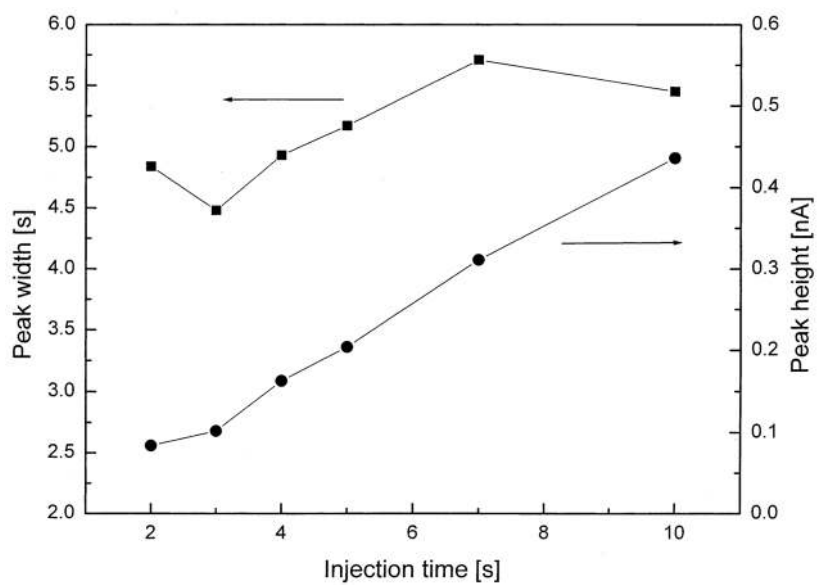


**Figure 5.** Effect of the injection time on the peak height and peak width. Experimental conditions as in Figure 4.

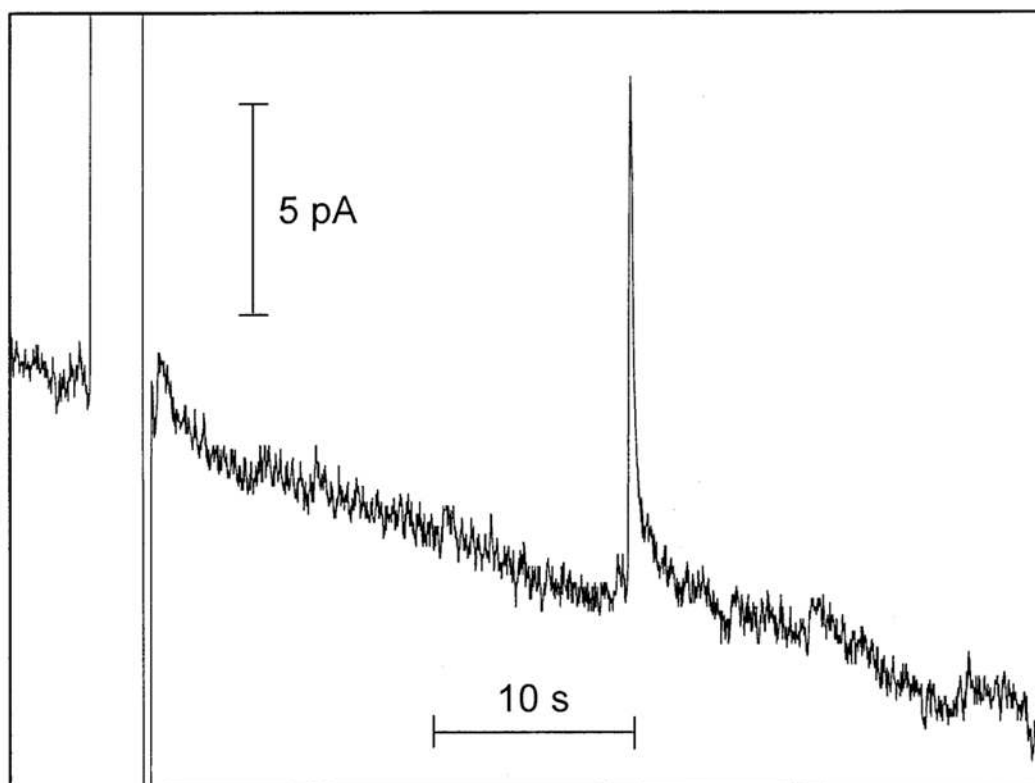


**Figure 6.** Electrochemical detection of ascorbic acid at a concentration close to the detection limit. Experimental conditions: analyte, 12  $\mu\text{M}$  ascorbic acid dissolved in 3.3 mM boric acid; background electrolyte, 10 mM boric acid; injection time, 5 s. Electrochemical detection: working electrode, 30  $\mu\text{m}$  carbon microdisk electrode; detection potential, 750 mV vs Ag-quasi reference electrode.



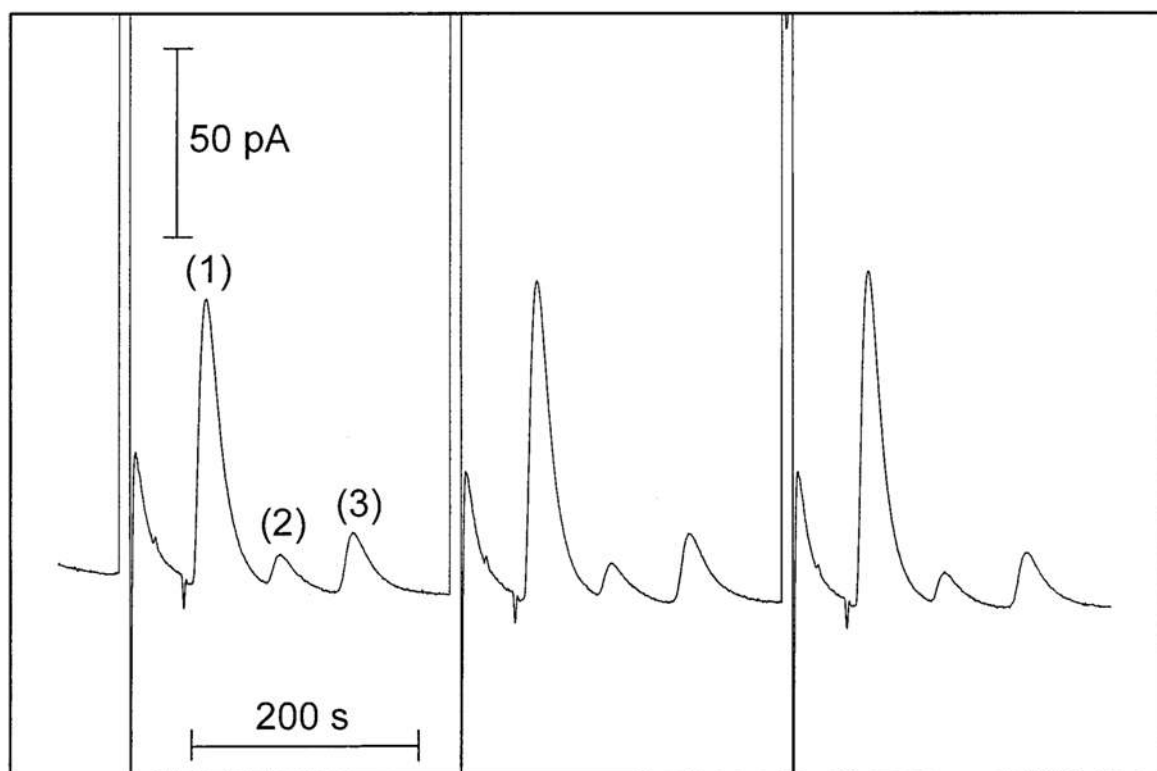


**Figure 7.** Microchip electrophoretic separation and electrochemical detection of physiologically relevant compounds: (1)  $1.0 \times 10^{-4}$  M noradrenaline, (2)  $1.0 \times 10^{-4}$  M L-dopa, and (3)  $2.5 \times 10^{-4}$  M ascorbic acid. Separation conditions: 10 mM boric acid, pH, 9.1; injection time, 10 s; high voltages, set at 1 (HV<sub>1</sub>) and 0.5 kV (HV<sub>2</sub>).

**Table 1**

High-Voltage Connections during Separation and Injections Steps Shown in Figure 3

Figure 3	mode of operation	HV <sub>1</sub> (1.2 kV)	HV <sub>2</sub> (1 kV)
a	separation	anode connected to B ground connected to D	anode connected to S cathode connected to SW
b	injection	turned off for $t_{inj} = 3$ s	turned off for $t_{inj} = 3$ s
c	separation	anode connected to B ground connected to D	anode connected to S cathode connected to SW